

Symplectic and antiplectic waves in an array of beating cilia attached to a curved body

Aref Ghorbani¹ and Ali Najafi^{1,2}

¹*Department of Physics, Institute for Advanced Studies in Basic Sciences (IASBS), Zanjan 45137-66731, Iran*

²*Physics Department, University of Zanjan, Zanjan 313, Iran**

(Dated: July 19, 2022)

By taking into account the hydrodynamic interactions in a one dimensional array of model cilia, attached to a curved no-slip surface, we investigate their synchronized motion. We show, how does the emergence of metachronal waves depend on the initial state of the system and investigate the conditions under which, the formation of symplectic and antiplectic waves are possible.

PACS numbers: 47.63.Gd, 87.16.Qp, 05.45.Xt

I. INTRODUCTION

Cillium, a micron scale flexible hair-like appendix, and their assembly, appear in many biological systems[1]. Mucus-ciliary transport in respiratory system and swimming of ciliated organisms like Volvox and Paramecium, are among the most important examples of cilia in biology [2–6]. In most of their natural appearance, the emergent synchronized motion of an assembly of many cilia is an essential key for their efficient performance. Using the forces from molecular motor-proteins, an individual cilium can beat independently[7]. It is mainly believed that the hydrodynamic interactions, can lead a collection of cilia to reach a synchronized state with propagating metachronal waves [8–10]. There are some experimental observations in artificial active colloidal systems that supports the idea of hydrodynamic mediated synchronization in colloidal systems[11, 12].

A metachronal wave is a kind of synchronized pattern of ciliary beating that results a traveling wave on the envelop of their tips. The average flow field due to the cyclic motion of an individual cilium is negligible but, a synchronized pattern of ciliary beating is able to either produce a net flow of the fluid in mucus or generate a swimming mechanism for the ciliated microorganisms. While maximum efficiency for synchronous motion with metachronal waves is expected [13–16], mechanism behind this wave pattern formation is not completely understood. Experimental studies, show that the direction of a metachronal wave can be either parallel (symplectic wave) or antiparallel (antiplectic wave) to the power-stroke direction of an individual cilia [5, 17].

There are many recent works that considered the problem of two or many cilia and investigated their synchronizations [18–24]. As to our knowledge, in most of the recent works, the curved geometry of the ciliated body is not considered. The roughness of the body has an essential influence on the hydrodynamic interactions. In this article we aim to study the emergence of metachronal waves in a collection of cilia attached to the peripheral

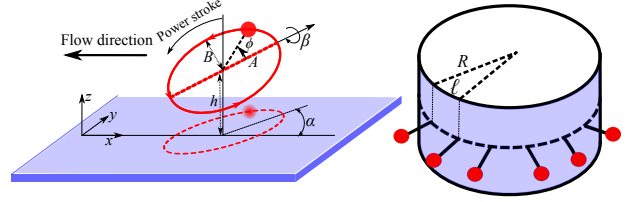


FIG. 1: Left: geometry of a single cilium, right: an array of cilia attached to the surface of a cylinder. The direction of power stroke and the average flow are shown in figure.

of a cylindrically curved body. For this purpose, we first introduce a simplified hydrodynamic model that can capture the hydrodynamics of a single cilium and then study the motion of their collection attached to a cylindrical body.

II. MODEL

In order to study the motion of an assembly of cilia, we start by defining our mechanical model for a single cilium. The ciliary motion composes of effective and recovery strokes that form an asymmetric cycle. As a result of such asymmetry, a cilium experiences different friction forces during its first and second semi cycles. This asymmetry is essential in allowing the cilium to produce a net flow of fluid along its stroke direction. It is shown that the flow pattern associated to a beating cilium can be modeled by the flow corresponding to a rigid sphere moving along an elliptic trajectory near a rigid and no-slip wall [18, 25]. The sphere resembles the hydrodynamic center of the cilium and the wall stands for the body on which cilium has been attached. To introduce the geometrical characteristics of a single cilium, let us start with a cilium attached to a flat wall. Fig. 1 shows a schematic view of the model and its geometrical parameters. In a reference frame located on the wall, the elliptic orbit is characterized by 6 parameters, A , B , h , x , α and β . The lengths of semi-major and semi-minor axes are denoted by A and B and the position vector of the center of ellipse is given by $(x, 0, h)$. The rigid wall is placed at $z = 0$. The plane of the ellipse and the rigid wall are

*Electronic address: najafi@iasbs.ac.ir

not parallel, the plane of ellipse is rotated with an angle β around its semi-major axis. Projecting the orbit on the plane, the semi-major axis is tilted with an angle α with respect to x -axis. For later use we denote the eccentricity of the orbit by $e = \sqrt{1 - (B/A)^2}$. Instantaneous dynamical state of the sphere moving on this orbit, is denoted by an angle $\phi(t)$.

Based on an intuitional argument, we can easily distinguish the direction of average flow produced by a cilium. To have a net flow, it is essential to have a tilted elliptic trajectory ($\beta \neq 0$). Motion of sphere in a part of the trajectory that is far from the wall, determines the flow direction, thus the flow pattern is in the same direction as the sphere has in its motion when it is far from wall. For a typical trajectory shown in fig. 1, the direction of the flow points from right to left.

In this article we aim to investigate the curvature of the ciliated body and its role in the dynamic of cilia. In order to attack this problem, we consider a 1 dimensional array of \mathcal{N} cilia, attached to a circle around the cylinder. The circle is wrapped around the cylinder and it has the same radius R as cylinder. As shown in fig. 1, two adjacent cilia are connected with an arc length $\ell = 2\pi R/\mathcal{N}$. The geometrical parameters of each cilia can be expressed with respect to a flat wall that is locally tangent to the cylinder. In the case that the length of each cilium, is comparable with this arc-length, we expect to see hydrodynamical effects due to the curvature of body. In the next section we will summarize all of the equations that are necessary to describe the dynamics of a coupled system of cilia.

III. DYNAMICAL EQUATIONS

Let us consider two cilia, each represented by a moving sphere with radii a and position vectors given by \mathbf{r}_i ($i = 1, 2$) and corresponding parameters for their elliptic trajectories. Hereafter we consider similar cilia that have same geometrical and dynamical properties. At micrometer scale where the dissipative effects dominate over inertial effects, it is a known fact that the governing equations for two interacting colloidal particles (here two cilia) can be written as linear relations between the i 'th particle's velocity $\mathbf{v}_i = \dot{\mathbf{r}}_i$ and the hydrodynamic forces acting on particles denoted by \mathbf{f}_j . In terms of their Cartesian components, we have:

$$v_{i,\mu} = \sum_{\nu=1}^3 \sum_{j=1}^2 G_{\mu\nu}(\mathbf{r}_i, \mathbf{r}_j) f_{j,\nu} \quad (1)$$

where Greek letters denote the cartesian components of the vectors. The hydrodynamic kernel $G_{\mu\nu}$ contains information about the geometry of the system: radii of spheres, their separation and their distances to the wall. Assuming that the sphere radius, a , is much smaller than all other lengths in system, we can write an approximate

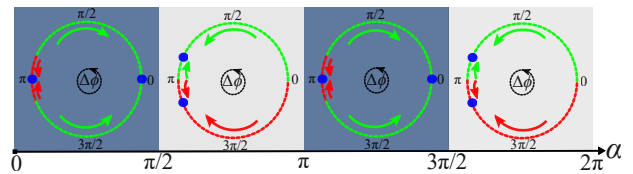


FIG. 2: Synchronization of two cilia depends on initial phase difference $\Delta\phi(0)$ and α . Different values of $\Delta\phi(0)$ are shown by points on a unit circle. The synchronized states of two cilia are represented by the long time value of their phase differences, $\Delta\phi(\infty)$, and are shown by bolded dots on the circles. Numerical parameters are: $a/h = 0.2$, $h/\ell = 0.19$, $B/\ell = 0.19$, $\beta = \pi/4$ and $e = 0.87$.

form for the component of the hydrodynamic kernel in a semi infinite domain confined by a rigid wall. For $\mathbf{r}_i \neq \mathbf{r}_j$, we have [26]:

$$G(\mathbf{r}_i, \mathbf{r}_i) \simeq \frac{3}{2\pi\eta} \frac{z_i z_j}{d^3} \begin{pmatrix} \cos^2 \psi & \sin \psi \cos \psi & 0 \\ \sin \psi \cos \psi & \cos^2 \psi & 0 \\ 0 & 0 & 0 \end{pmatrix}, \quad (2)$$

where η is the fluid viscosity, $z_i = \hat{z}_i \cdot \mathbf{r}_i$, $d = \sqrt{(x_j - x_i)^2 + (y_j - y_i)^2}$ and we have assumed that $z_i, z_j \ll d$. Here ψ is defined as: $\tan \psi = (y_j - y_i)/(x_j - x_i)$. For $\mathbf{r}_i = \mathbf{r}_j$, we have:

$$G(\mathbf{r}_i, \mathbf{r}_i) \simeq \frac{1}{6\pi\eta a} \begin{pmatrix} 1 - \epsilon & 0 & 0 \\ 0 & 1 - \epsilon & 0 \\ 0 & 0 & 1 - 2\epsilon \end{pmatrix} \quad (3)$$

where $\epsilon = (9a/16z)$. Let us continue our discussion about the case of two interacting cilia near a flat wall, then we will show how the effects due to the curvature of the body can be considered. In addition to the above hydrodynamic equations, we should provide some information about the internal forces inside each cilium that drive its beating. In addition to constraining forces that enforce the particle to move on elliptic orbit, there is also tangential force that results the motion along orbit. Denoting the unit vector tangent to the trajectory by $\hat{\mathbf{t}}$, the tangential component of the force reads as: $f_t = \hat{\mathbf{t}} \cdot \mathbf{f}$. In general, the tangential force is related to the velocity of sphere along its trajectory $v_t = \hat{\mathbf{t}} \cdot \mathbf{v}$. In linear response regime, an equation like $f_t = f_0(1 - v_t/v_0)$ captures the dynamics of a cilium. Here f_0 is the stall force and it is the amount of external force necessary to stop the motion of a beating cilium. A free cilium that is not affected by any external force, moves with velocity $v_t = v_0$. In this linear response approximation, two parameters f_0 and v_0 are related to the microscopic details of the cilium. Defining the stiffness of the cilium by $\kappa = f_0/6\pi\eta a v_0$, we will use a numerical value for this parameter as $\kappa = 0.1$ [27].

Let us now explain how can we take into account the curvature effects. In order to study the curvature, the hydrodynamic kernel should be replaced. In a confined space that is limited by a curved wall, the above men-

tioned kernel is no longer valid. We proceed by an approximate scheme to consider the curvature effects. Here we assume that for two neighboring cilia, there is an effective plane that can be used for constructing the image system. This effective wall, is a wall that is locally tangent to the curved body at the mid point of two cilia. We can use the results of flat-wall confinement, to obtain the approximate interaction between two adjacent cilia. It is obvious that with this approximation, we do not expect to see any curvature effect in the motion of two cilia. The curvature, in this approximation, has no effect on the dynamics of two cilia. This approximation can only include non trivial curvature effects to the motion of many cilia (more than two), attached to the cylinder. The validity of this approximation is guaranteed for the case where $h \gg \ell$, this is also the case of real situation in ciliated body.

To obtain the dynamics of two coupled cilia, one should note that in a way that we have parametrized the orbits, the kinematics of each cilium can be expressed by a single phase denoted by $\phi_i(t)$. This phase variable is shown in fig. 1. Solving the dynamical equations and applying the geometrical and dynamical constraints, we will arrive at the following equations:

$$\dot{\phi}_i(t) = g_1(\phi_i)\omega_0 + g_2(\phi_i, \phi_j). \quad (4)$$

Here $\omega_0 = f_0/(6\pi\eta aB(1 + \kappa))$ and the interaction between cilia are reflected by function g_2 that couples the dynamics of phases. It is not possible to present analytical closed relations for functions g_1 and g_2 but, in principle we are able to evaluate and study them numerically. In the next section, we will summarize the results of numerical investigations of the above equations.

IV. RESULTS AND DISCUSSION

Before studying the wave propagation in ciliated curved body, we consider the dynamics of two coupled cilia. Recalling the geometry of elliptic orbits, angles α and β , play important role in the dynamics of coupled cilia. Numerical solutions to the equations for two interacting cilia, show that for $\beta = 0$ and $\beta = \pi/2$ (orbits are parallel and perpendicular to the wall respectively), the long time dynamics of cilia does not show any correlations in their beating patterns. In this case, the hydrodynamic mediated interactions between two cilia, act in an incoherent way and the state of motion for each cilium is independent from the other. This result is consistent with previous works of beating cilia near a flat wall [28, 29]. When elliptic orbits are tilted ($\beta \neq 0, \pi/2$), temporal correlations in the long time dynamics of interacting cilia will appear. Our numerical studies show that for tilted orbits, the cilia reach a phase-locked synchronized state. At this synchronized state, the phase difference $\Delta\phi(t) = \phi_2(t) - \phi_1(t)$ reaches a constant value that we will denote it by $\Delta\phi(\infty)$. The steady state phase

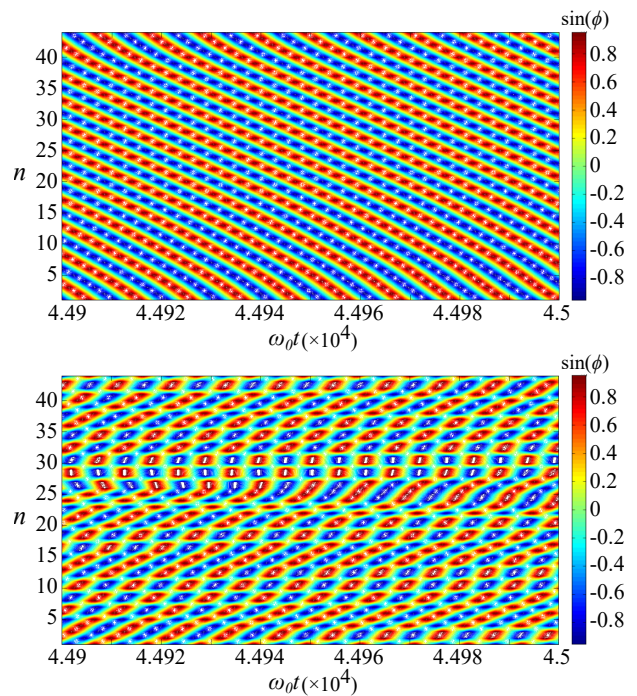


FIG. 3: State of synchronization in a collection of cilia can be seen in a time-phase portrait. The vertical axes shows the cilium number n , the horizontal axis show the time and the value of $\sin(\phi_n(t))$ are encoded via colors. Symplectic wave appears for $\alpha = 2\pi - \frac{\pi}{4}$ (up) and antiplectic wave appear for $\alpha = \frac{\pi}{4}$ (down). The numerical parameters are $a/h = 0.2$, $h/\ell = 0.35$, $B/\ell = 0.22$, $e = 0.87$ and $\beta = \pi/4$.

difference, $\Delta\phi(\infty)$, depends on initial conditions, the angle of ellipse α and also e . Fig. 2, shows the state of synchronization and its dependence to α and $\Delta\phi(0)$ for $e \neq 0 (= 0.87)$. As one can see from this figure, for $0 < \alpha < \pi/2$ and $\pi < \alpha < 3\pi/2$, depending on the initial phase difference between cilia, the final state can be either $\Delta\phi(\infty) = 0$ or $\Delta\phi(\infty) = \pi$. Behavior for other values of α and its sensitivity to the initial phase difference can be seen at the figure. For $\pi/2 < \alpha < \pi$ and $3\pi/2 < \alpha < 2\pi$, $\Delta\phi(\infty)$ approaches to a constant value, $\pi + \delta$, where depending on the initial phase difference, δ could be also a positive or negative small angle. The synchronization picture shown in fig. 2, is valid for any $e \neq 0$. For a special case of $e = 0$ where, the orbits are circular, and for $0 < \alpha < \pi/2$ and $\pi < \alpha < 3\pi/2$, we observed that the two cilia system reaches a synchronized state with $\Delta\phi(\infty) = 0$. When $e = 0$ and for $\pi/2 < \alpha < \pi$ and $3\pi/2 < \alpha < 2\pi$, the systems reaches to a state with $\Delta\phi(\infty) = \pi$.

Let us examine the dynamics of a one dimensional array of $\mathcal{N} = 44$ cilia, attached to the circumference of a cylinder. We take into account the nearest neighbor hydrodynamic interactions and considered both cases of elliptic and circular orbits separately ($e = 0$ and $e = 0.87$). Interestingly, unlike the case of two cilia, the emergence of synchronized states, does not show any dependence

on the value of e . Fig. 3, shows two examples for the time evolution of the phase variables for all cilia. The phase values are encoded via colors. The patterns shown in this figure, demonstrate the long time dynamics of the system. The regularity of the long time patterns, reflects the temporal correlations in the motion of cilia. In this case, a traveling metachronal wave, shows a synchronized state of the cilia [8, 29, 30]. For a propagating wave (metachronal wave) in the array of cilia, the phase of n 'th cilium $\phi_n(t)$ can be written as: $\phi_n(t) = nK - \Omega t$, where the number K plays the role of a wave number associated with metachronal wave. In a regular patterns shown in fig. 3, the regions with constant phases (same colors) make straight lines. These straight lines are given by an equation like: $nK = \Omega t + C$, where C is a constant. The slope of these parallel lines, measures the wavelength of a metachronal wave and it is given by $1/K = \partial n / \partial(\Omega t)$. For $K > 0$, the wave moves in a direction with increasing cilium's number n . As shown in fig. 1, the flow direction is always points to the left (from large n to small n cilia). So we conclude that, positive slope corresponds to antiplectic and negative slope shows a symplectic metachronal wave. Fig. 3, show two example of metachronal waves for $\alpha = \pi/4$ and $\alpha = 2\pi - \pi/4$. As one can see, in the first case (fig. 3(up)), a symplectic wave has appeared, and for the second case (fig. 3(down)), an antiplectic wave has appeared. Our numerical investigations show that, the emergence of such synchronized states (simplectic and

antiplectic), crucially depends on the value of α . Independent of the value of e , the symplectic metachronal waves appear for $0 < \alpha < \pi/2$ and $\pi < \alpha < 3\pi/2$. On the other hand, antiplectic metachronal waves appear when $\pi/2 < \alpha < \pi$ and $3\pi/2 < \alpha < 2\pi$. Changing α to $2\pi - \alpha$, the average direction of the fluid flow does not change but the propagation direction of the metachronal wave will change. Comparing the results for an array of cilia with the results of two cilia, one can see that the emergence of symplectic or antiplectic synchronization in an array of cilia, is directly related to the state of synchronization in the case of two cilia.

In conclusion, the state of synchronization is studied for interacting cilia. For two cilia, the synchronized state depends on the initial phase difference and the geometrical parameters given by α and β . In-phase, anti-phase ($\delta\phi = 0, \pi$) synchronized states have been observed. For a $1-D$ array of cilia attached to a curved body, we found that, both symplectic and antiplectic metachronal waves can appear. The emergence of symplectic and antiplectic waves in an array of cilia, is in direct connection with the state of synchronization in two cilia case. As a result of our study, we understand the the geometrical characteristics are key elements in determining the state of metachronal waves. The emergence of symplectic or antiplectic metachronism in our model is not an artifact of imposing closed boundary condition. The boundary condition in our system, emerges naturally from the closed structure of the curved body.

-
- [1] B. Alberts, A. Johnson, J. Lewis, K. Roberts, M. Raff, and P. Walter, *Molecular Biology of the Cell*, Molecular Biology of the Cell (Garland Science, 2002), ISBN 9780815332183.
- [2] J. Blake, *Journal of Fluid Mechanics* **46**, 199 (1971).
- [3] A. Dummer, C. Poelma, M. C. DeRuiter, M.-J. T. Goumans, and B. P. Hierck, *Cilia* **5**, 1 (2016).
- [4] D. B. Hill, V. Swaminathan, A. Estes, J. Cribb, E. T. O'Brien, C. W. Davis, and R. Superfine, *Biophysical Journal* **98**, 57 (2010).
- [5] G. Witzany and M. Nowacki, *Biocommunication of ciliates* (Springer, 2016).
- [6] C. Brennen and H. Winet, *Annual Review of Fluid Mechanics* **9**, 339 (1977).
- [7] I. H. Riedel-Kruse, A. Hilfinger, J. Howard, and F. Jülicher, *HFSP journal* **1**, 192 (2007).
- [8] S. Gueron and K. Levit-Gurevich, *Biophysical Journal* **74**, 1658 (1998).
- [9] M. Lighthill, *Communications on Pure and Applied Mathematics* **5**, 109 (1952).
- [10] A. Najafi and R. Golestanian, *EPL (Europhysics Letters)* **90**, 68003 (2010).
- [11] J. Kotar, M. Leoni, B. Bassetti, M. C. Lagomarsino, and P. Cicuta, *Proceedings of the National Academy of Sciences* **107**, 7669 (2010).
- [12] R. Di Leonardo, A. Búzás, L. Kelemen, G. Vizsnyiczai, L. Oroszi, and P. Ormos, *Physical review letters* **109**, 034104 (2012).
- [13] S. Gueron and K. Levit-Gurevich, *Proceedings of the National Academy of Sciences* **96**, 12240 (1999).
- [14] S. Michelin and E. Lauga, *Physics of Fluids (1994-present)* **22**, 111901 (2010).
- [15] N. Osterman and A. Vilfan, *Proceedings of the National Academy of Sciences* **108**, 15727 (2011).
- [16] K. Ishimoto and E. A. Gaffney, *Physical Review E* **90**, 012704 (2014).
- [17] E. Knight-Jones, *Quarterly Journal of Microscopical Science* **3**, 503 (1954).
- [18] A. Vilfan and F. Jülicher, *Phys. Rev. Lett.* **96**, 058102 (2006).
- [19] N. Uchida and R. Golestanian, *Physical Review Letters* **106**, 058104 (2011).
- [20] H. Stark and M. Reichert, *Journal of Biomechanics* **39**, S349 (2006).
- [21] J. Elgeti and G. Gompper, *Proceedings of the National Academy of Sciences* **110**, 4470 (2013).
- [22] D. R. Brumley, M. Polin, T. J. Pedley, and R. E. Goldstein, *Journal of The Royal Society Interface* **12** (2015), ISSN 1742-5689.
- [23] B. Qian, H. Jiang, D. A. Gagnon, K. S. Breuer, and T. R. Powers, *Physical Review E* **80**, 061919 (2009).
- [24] R. Golestanian, J. M. Yeomans, and N. Uchida, *Soft Matter* **7**, 3074 (2011).
- [25] B. Guirao and J.-F. Joanny, *Biophysical journal* **92**, 1900 (2007).
- [26] C. Pozrikidis, *Boundary integral and singularity methods*

- for linearized viscous flow* (Cambridge University Press, 1992).
- [27] J. Howard, *Mechanics of Motor Proteins and the Cytoskeleton* (Sinauer Associates, Publishers, 2001), ISBN 9780878933341.
- [28] P. Lenz and A. Ryskin, *Physical Biology* **3**, 285 (2006).
- [29] T. Niedermayer, B. Eckhardt, and P. Lenz, *Chaos: An Interdisciplinary Journal of Nonlinear Science* **18**, 037128 (2008).
- [30] D. R. Brumley, M. Polin, T. J. Pedley, and R. E. Goldstein, *Phys. Rev. Lett.* **109**, 268102 (2012).